Supplementary Figure Legend

Supplementary Figure 1. Survival comparisons between HCC patients stratified by TP53 mutational status. (A) The Overall survival of patients in *TP53* MT and WT group. The Kaplan-Meier plot as well as number of patients at risk for each group was shown. (B) Similar with (A), but using Disease-specific survival information.

Supplementary Figure 2. The intersection of up-regulated differentially expressed genes identified by the three methods. (A) Up-regulated DEMs in *TP53* MT group. (B) Up-regulated DEMs in *TP53* WT group. (C) Up-regulated DELs in *TP53* MT group. (D) Up-regulated DELs in *TP53* WT group. (E) Up-regulated DEmis in *TP53* MT group. (F) Up-regulated DEmis in *TP53* WT group.

Supplementary Figure 3. The intersection of down-regulated differentially expressed genes identified by the three methods. (A) Down-regulated DEMs in *TP53* MT group. (B) Down-regulated DEMs in *TP53* WT group. (C) Down-regulated DELs in *TP53* MT group. (D) Down-regulated DELs in *TP53* WT group. (E) Down-regulated DEmis in *TP53* MT group. (F) Down-regulated DEmis in *TP53* WT group.

Supplementary Figure 4. Enrichment analysis on DEMs identified from TP53 WT HCC samples. (A) GO Biological Process enrichment analysis results. The enriched terms for up-regulated and down-regulated DEMs were marked with red and cyan colors. (B) Similar with (A), but using KEGG database. (C) Similar with (A), but using Reactome database.

Supplementary Figure 5. Survival analysis on patients stratified by expressions of ceRNA network nodes. (A-C) Kaplan–Meier survival curves showed the overall survival of patients stratified by high/low (A) AC017104.6, (B) RP5-1092A11.5 and (C) RP11-365O16.6 expression. (D) Heatmap illustrating the concomitant expressional patterns of ceRNA network nodes. (E-F) Kaplan–Meier survival curves showed the (E) overall survival and (F) disease-specific survival of patients stratified by high/low network node expression.

Supplementary Figure 6. Associations between expression of RP5-1092A11.5 and immune infiltrating cells in TP53 MT group. (A-D) Correlation analysis results on four cell types, including (A) Common lymphoid progenitor, (B) T cell CD4+ T helper (Th) 2, (C) T cell CD4+ memory and (D) Mast cell. Correlations were quantified by Spearman's rank correlation coefficients.

Supplementary Figure 7. Associations between expression of AC017104.6 and immune infiltrating cells in TP53 MT group. (A-D) Correlation analysis results on four cell types, including (A) Common lymphoid progenitor, (B) T cell CD4+ T helper (Th) 2, (C) T cell CD4+ memory and (D) Mast cell. Correlations were quantified by Spearman's rank correlation coefficients.

Supplementary Figure 8. Associations between expression of RP11-365O16.6 and immune infiltrating cells in TP53 MT group. (A-D) Correlation analysis results on four cell types, including (A) Common lymphoid progenitor, (B) T cell CD4+ T helper (Th) 2, (C) T cell CD4+ memory and (D) Mast cell. Correlations were quantified by Spearman's rank correlation coefficients.

Supplementary Figure 9. Comparisons on immune cell infiltrations between patients stratified by TP53 mutational status as well as survival analysis results incorporating tumor microenvironment difference. (A) Statistical differences of immune cell infiltrations in *TP53* MT and *TP53* WT group. Significantly different immune cell types were marked with cyan color

while types positively correlated with ceRNA network nodes were marked with red. Infiltration levels were compared using Wilcoxon rank sum test adjusted by Benjamini & Hochberg method. (B) Kaplan–Meier survival curve showed the overall survival of *TP53* MT patients with different infiltrations of T cell CD4+ T helper (Th) 2. (C) Similar with (B), but using disease-specific survival. (D) Similar with (B), but focusing on Mast cell. (E) Similar with (D), but using disease-specific survival. (F) Similar with (B), but focusing on T cell CD4+ memory. (G) Similar with (F), but using disease-specific survival.

Supplementary Figure 10. Relationship between cancer-immunity cycle activity and ceRNA network nodes. (A) Heatmap illustrating the correlations between cancer-immunity cycle steps and ceRNA network nodes in *TP53* MT patients. Clusters with high correlation values were marked with red rectangle. (B-E) Correlation analyses between the activity of "infiltration of immune cells into tumors" step and expressions of ceRNA network nodes in *TP53* MT group, including (B) *PTBP1*, (C) AC017104.6, (D) RP5-1092A11.5 and (E) RP11-365O16.6. Correlations were quantified by Spearman's rank correlation coefficients.

Supplementary Figure 11. Correlation between chemotherapy resistance-related genes and the expression of ceRNA network nodes. (A) Heatmap illustrating the correlations between chemoresistance genes and ceRNA network nodes in *TP53* MT patients. Clusters with high correlation values as well as the corresponding nodes were marked with red rectangle. (B) Expressions of *PTBP1*-associated chemoresistance genes in *TP53* MT, *TP53* WT and normal group.

Supplementary Figure 12. Dynamics on the DNA methylation level of PTBP1-related probes and their associations between DNA methylation regulators. (A) Line plot depicting the alternation trend of *PTBP1*-related probes with observable group-wise methylation difference. The only probe with methylation level inversely correlated with the expression trend of *PTBP1* was marked with red color. (B) The distribution of DNA methylation levels of probe cg02086742 probe in *TP53* MT, WT and normal group. (C-D) The distribution of two DNA methylation erasers' expression in *TP53* MT, WT and normal group, including (C) TET1 and (D) TET3 protein. Values were compared using Wilcoxon rank sum test. ns: not significant, *: p-value<=0.05; **: p-value<=0.01, ***: p-value<=0.001, ****: p-value<=0.0001.

Supplementary Figure 13. Distribution on the sensitivity of drugs better responded to TP53 WT group. (A-D) Comparisons on IC50 values of drugs with higher sensitivity in *TP53* WT patients, including (A) JQ1, (B) NU7441, (C) SB216763 and (D) ZM447439. Values were compared using Wilcoxon rank sum test. *: p-value<=0.05, ****: p-value<=0.0001.

Supplementary Figure 1

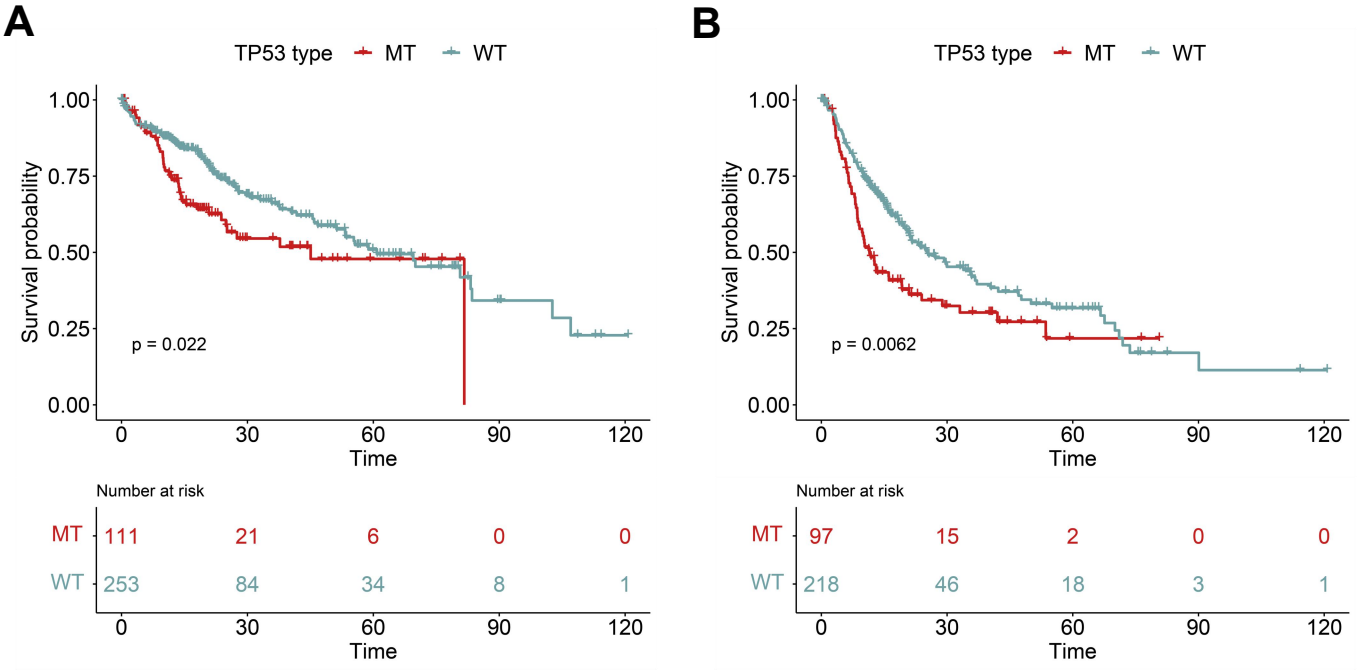

Supplementary Figure 2

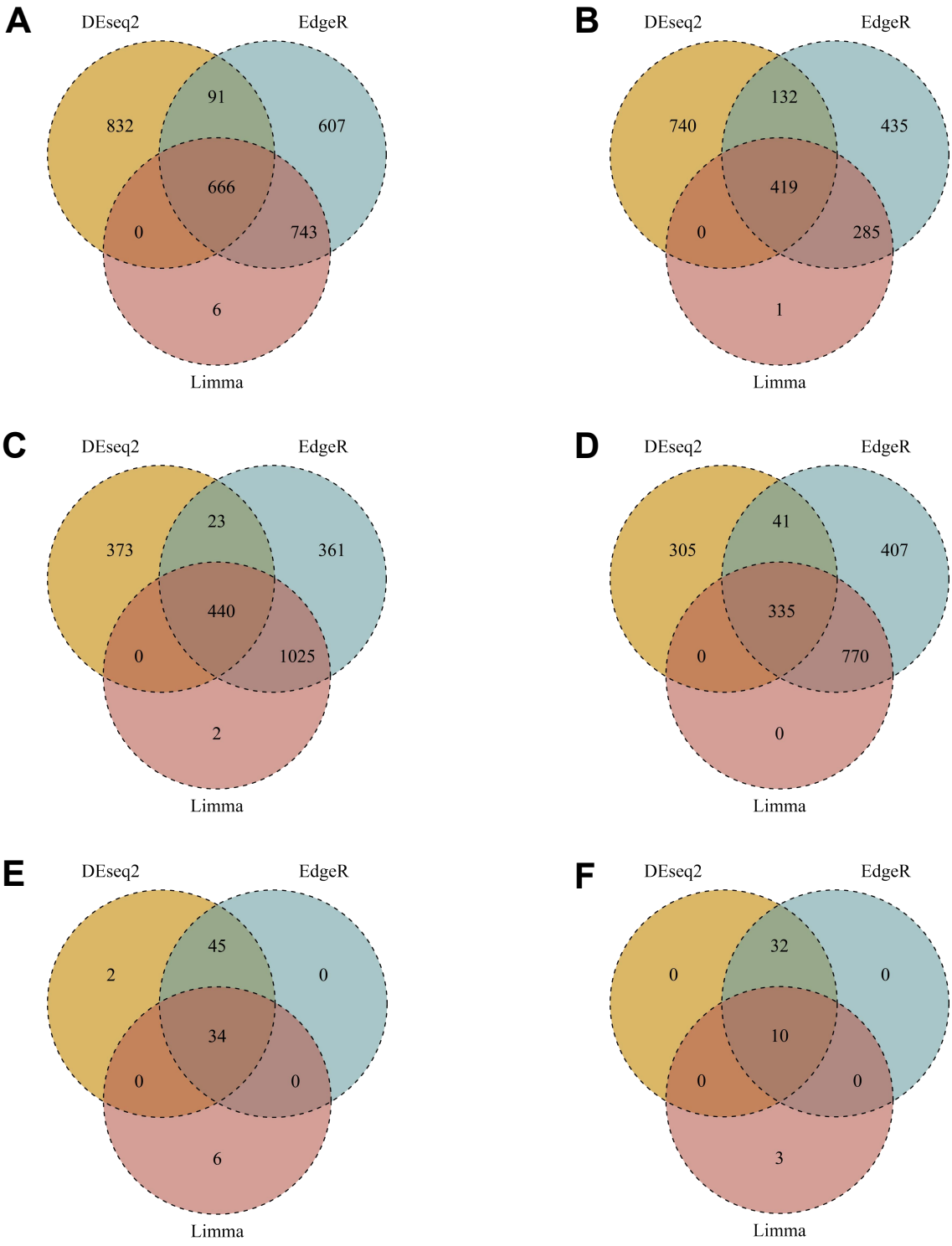

Supplementary Figure 3

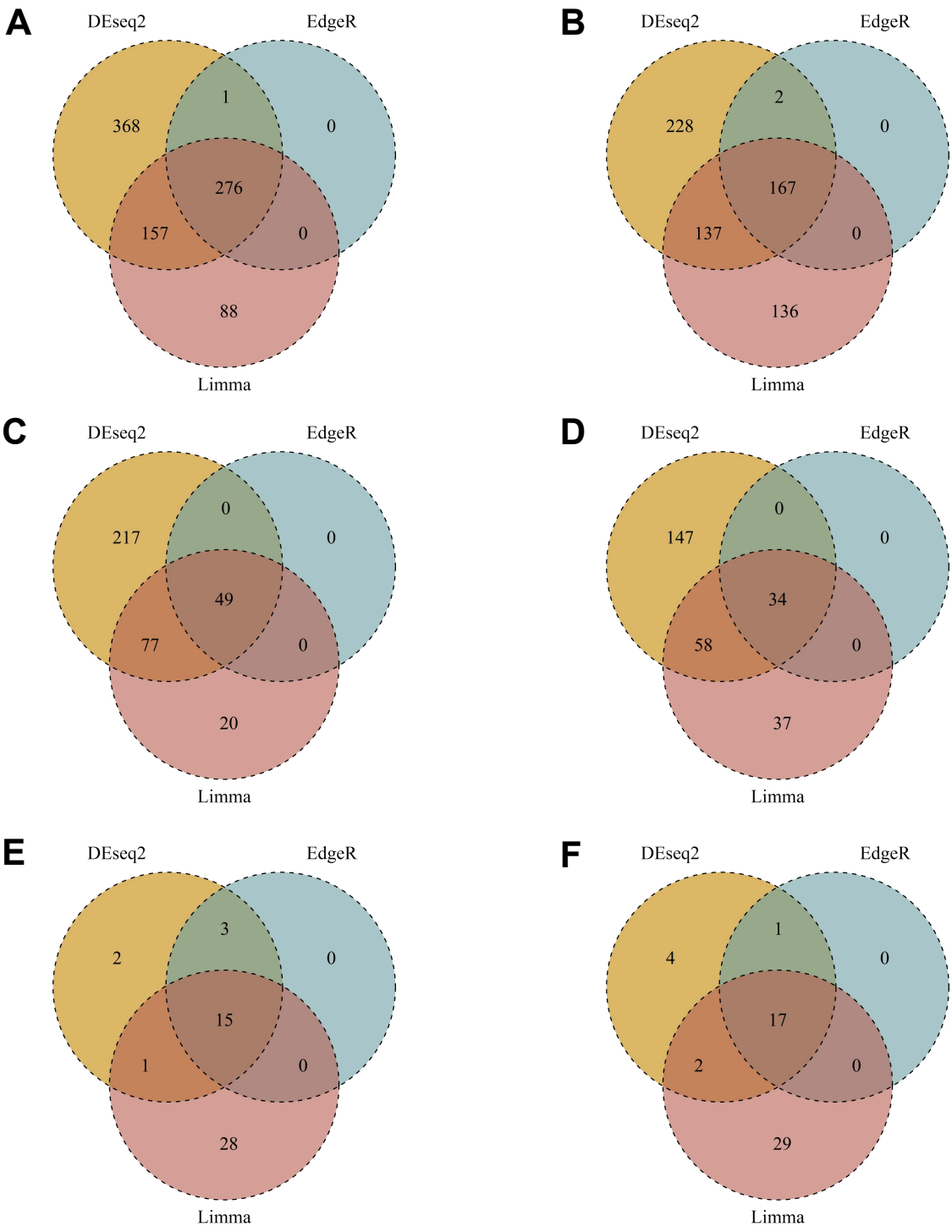

Supplementary Figure 4

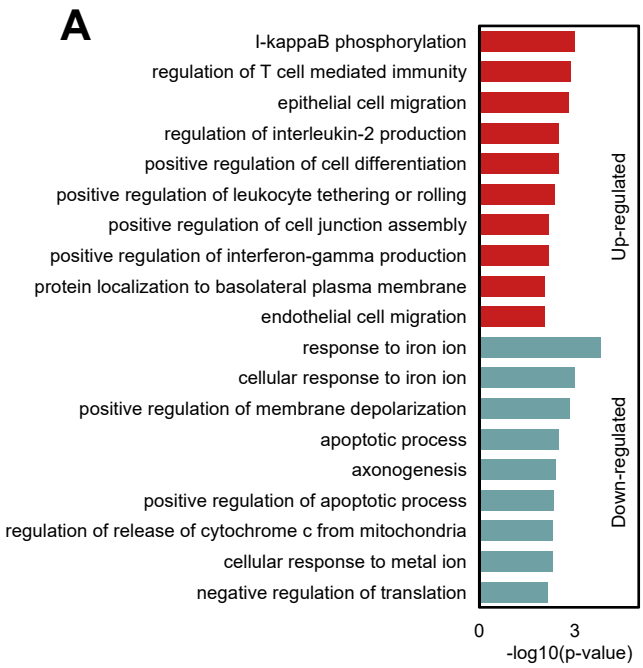

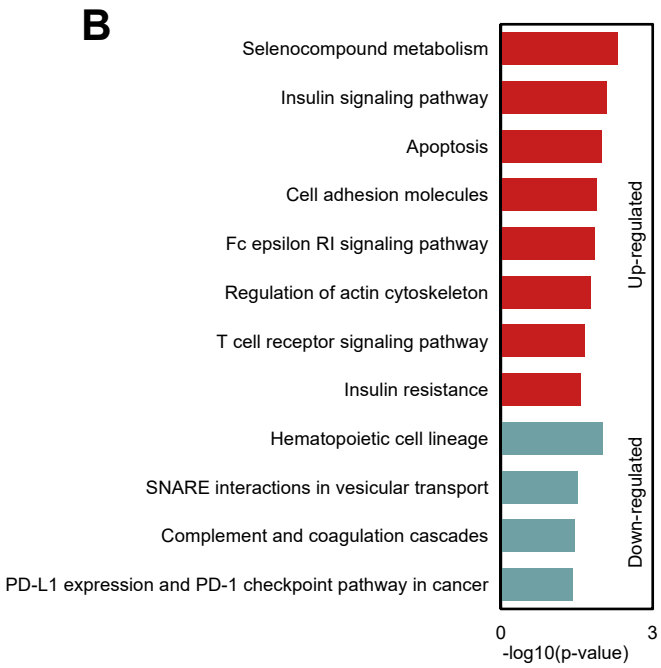

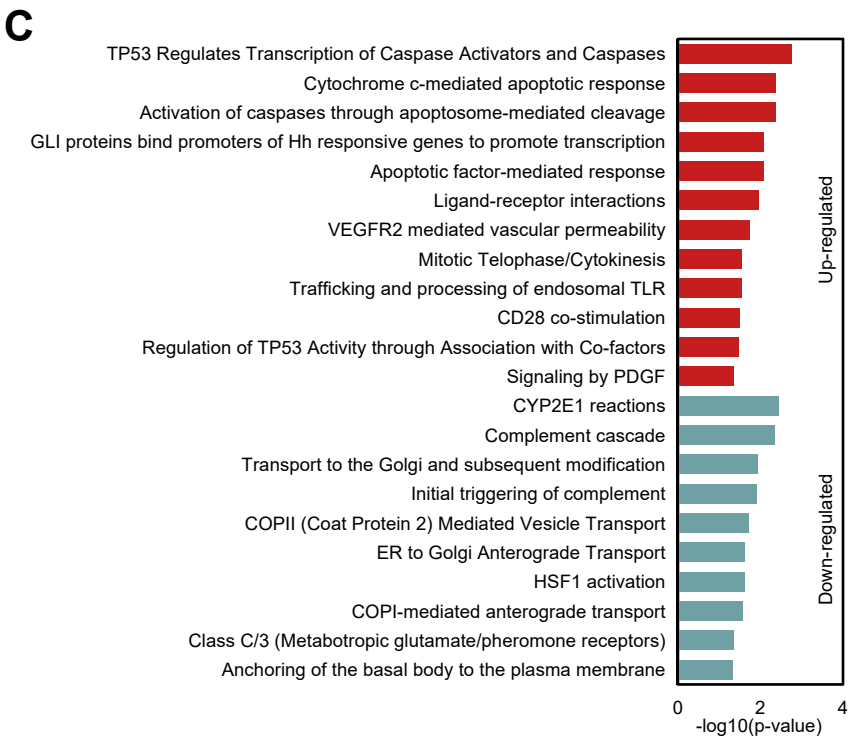

Supplementary Figure 5

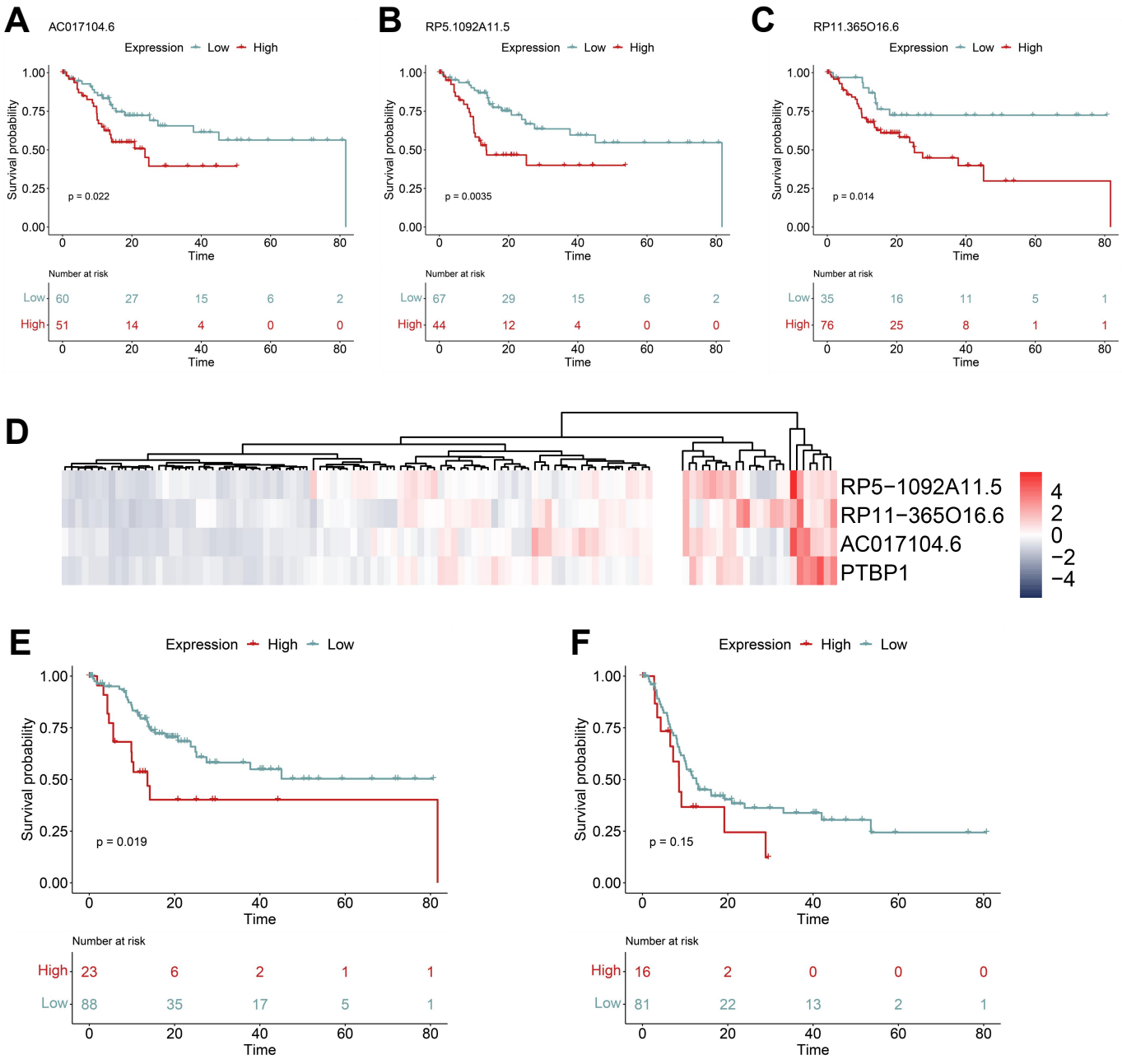

Supplementary Figure 6

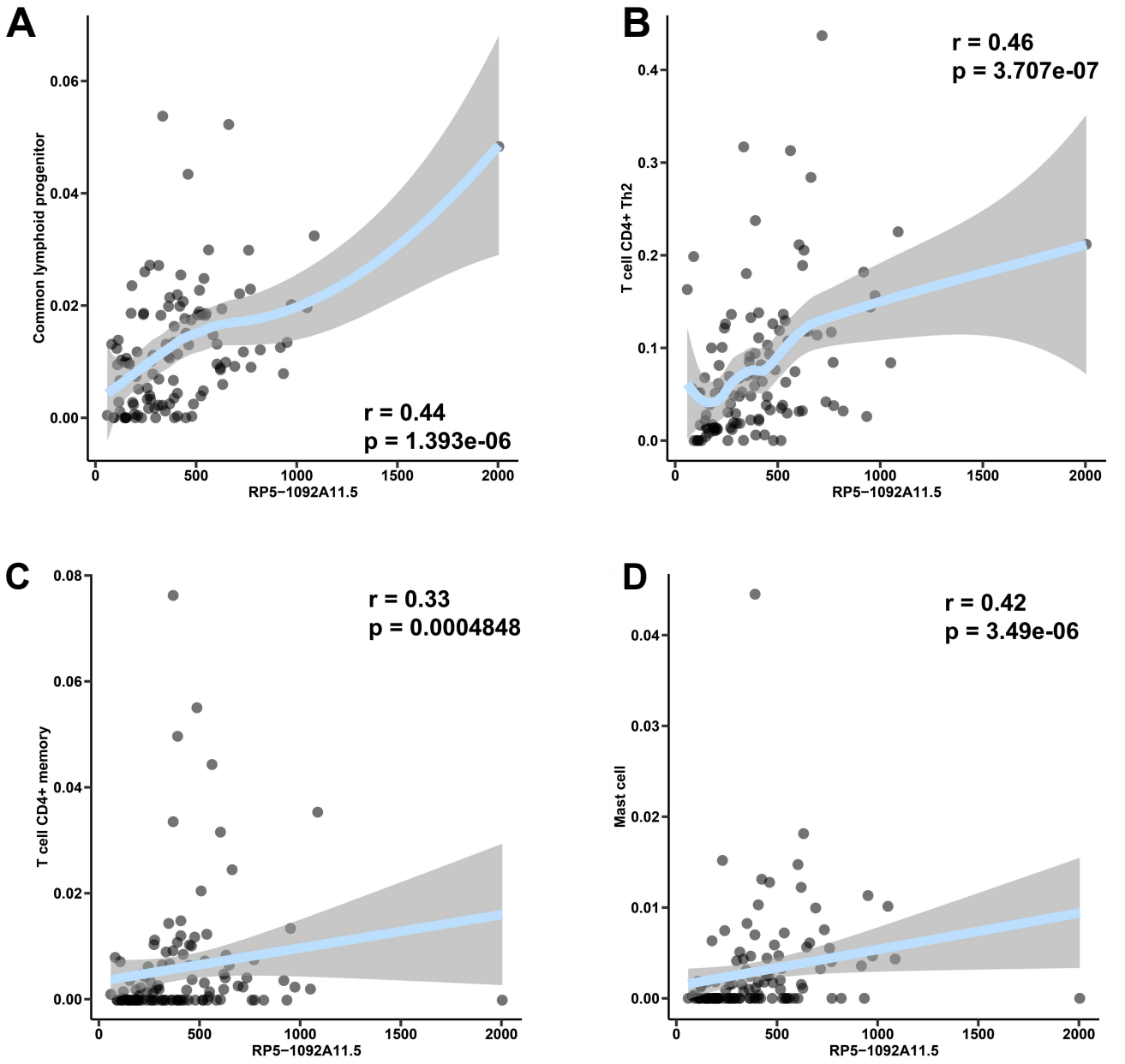

Supplementary Figure 7

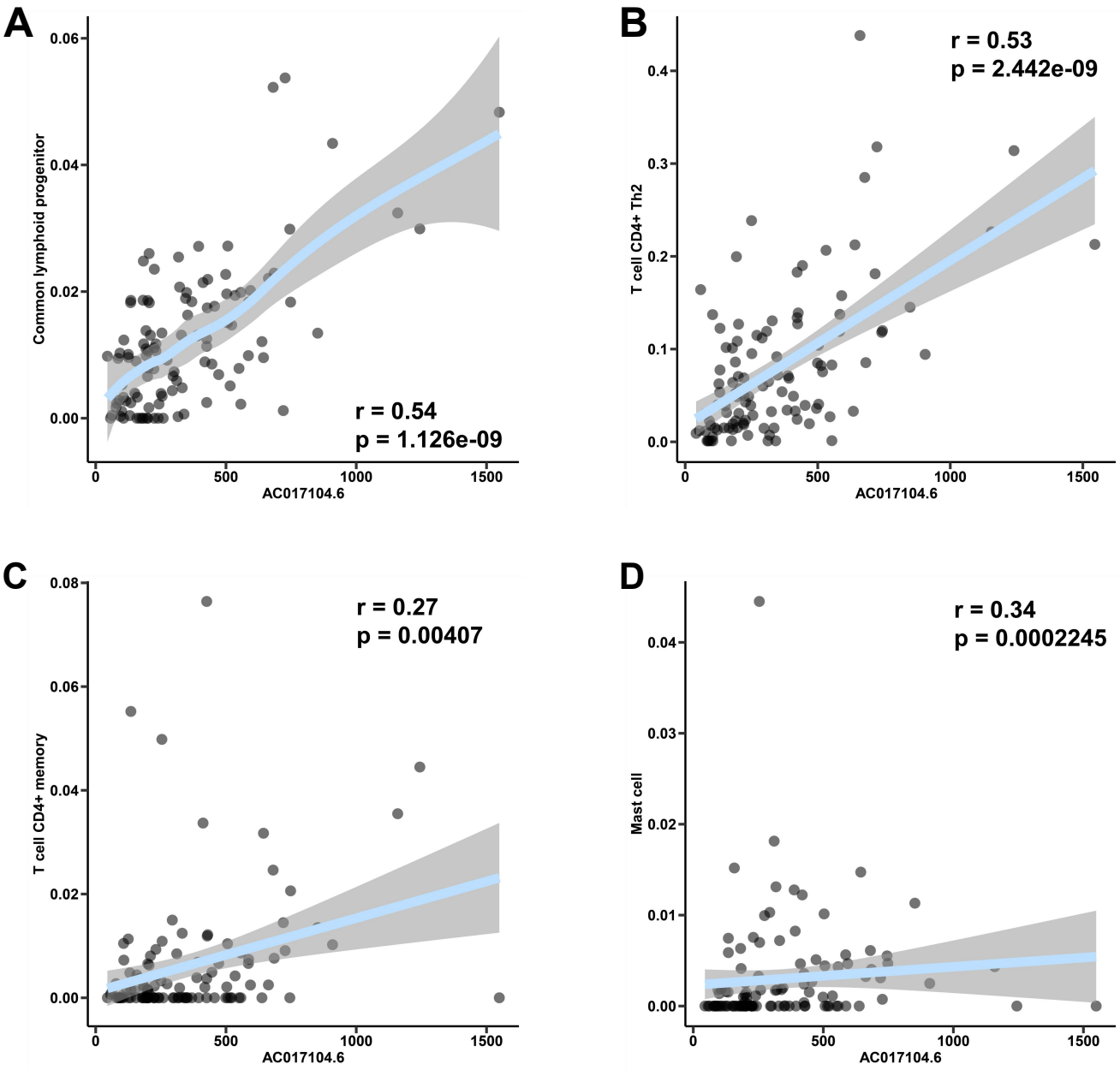

Supplementary Figure 8

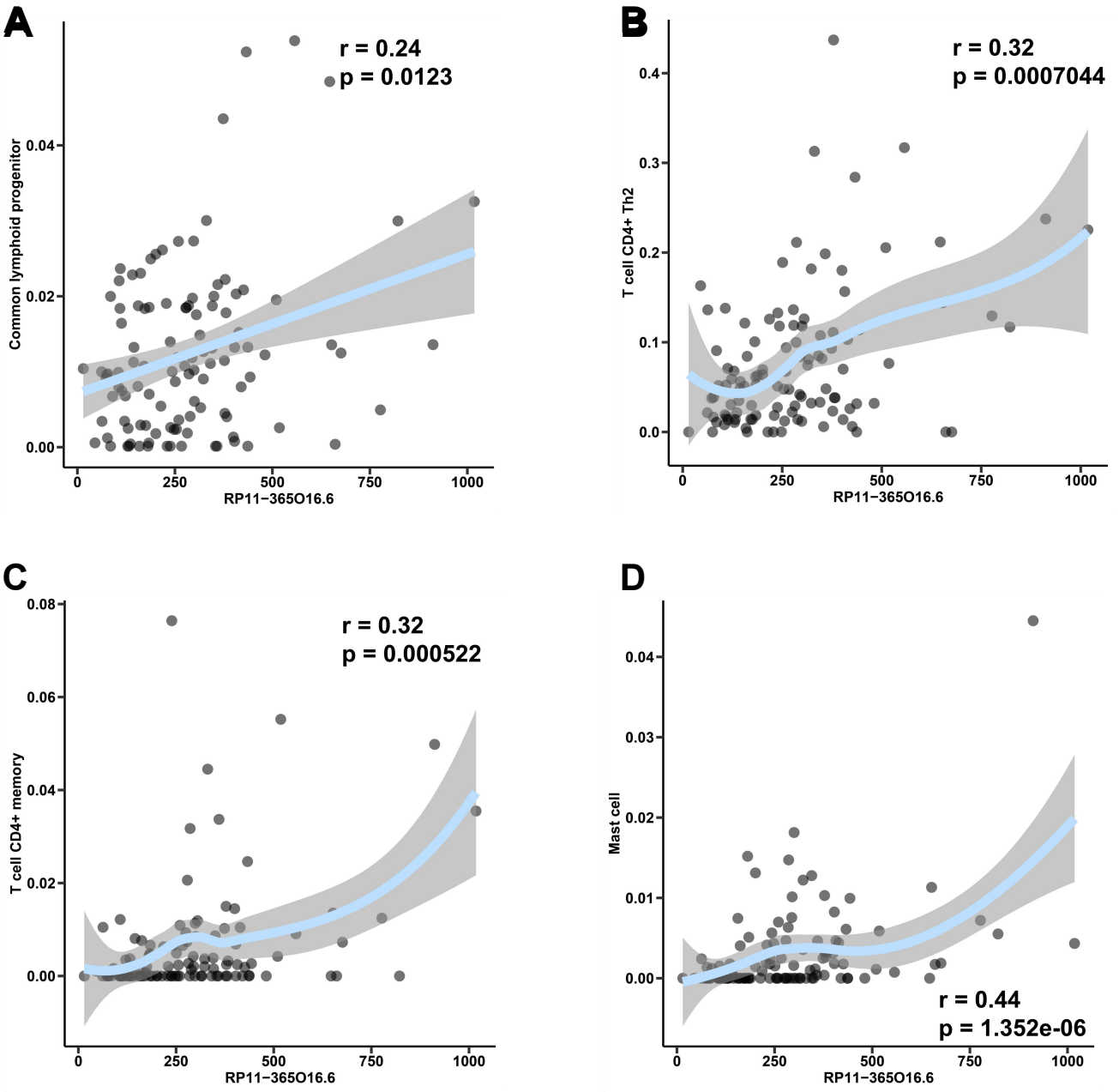

Supplementary Figure 9

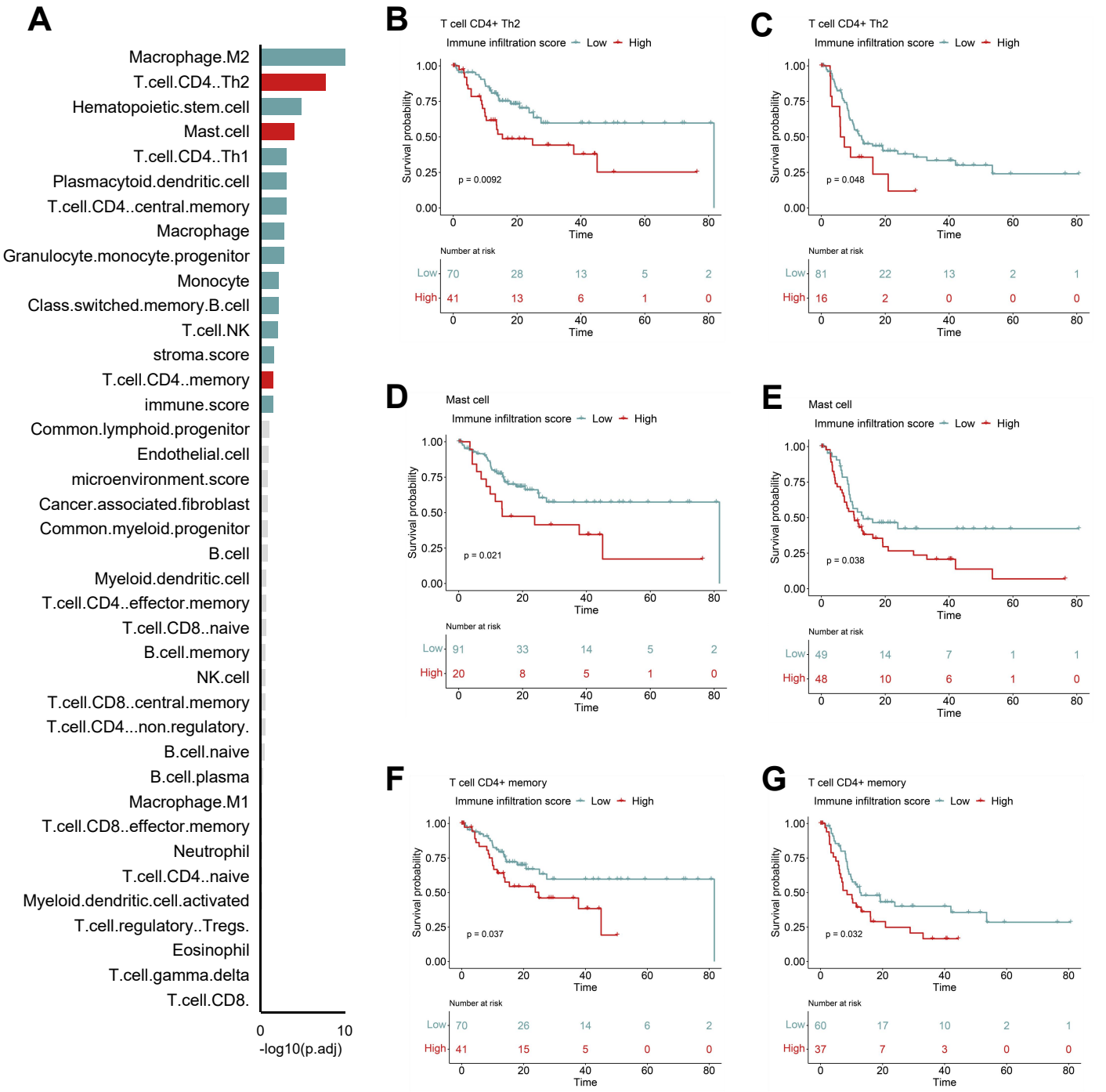

Supplementary Figure 10

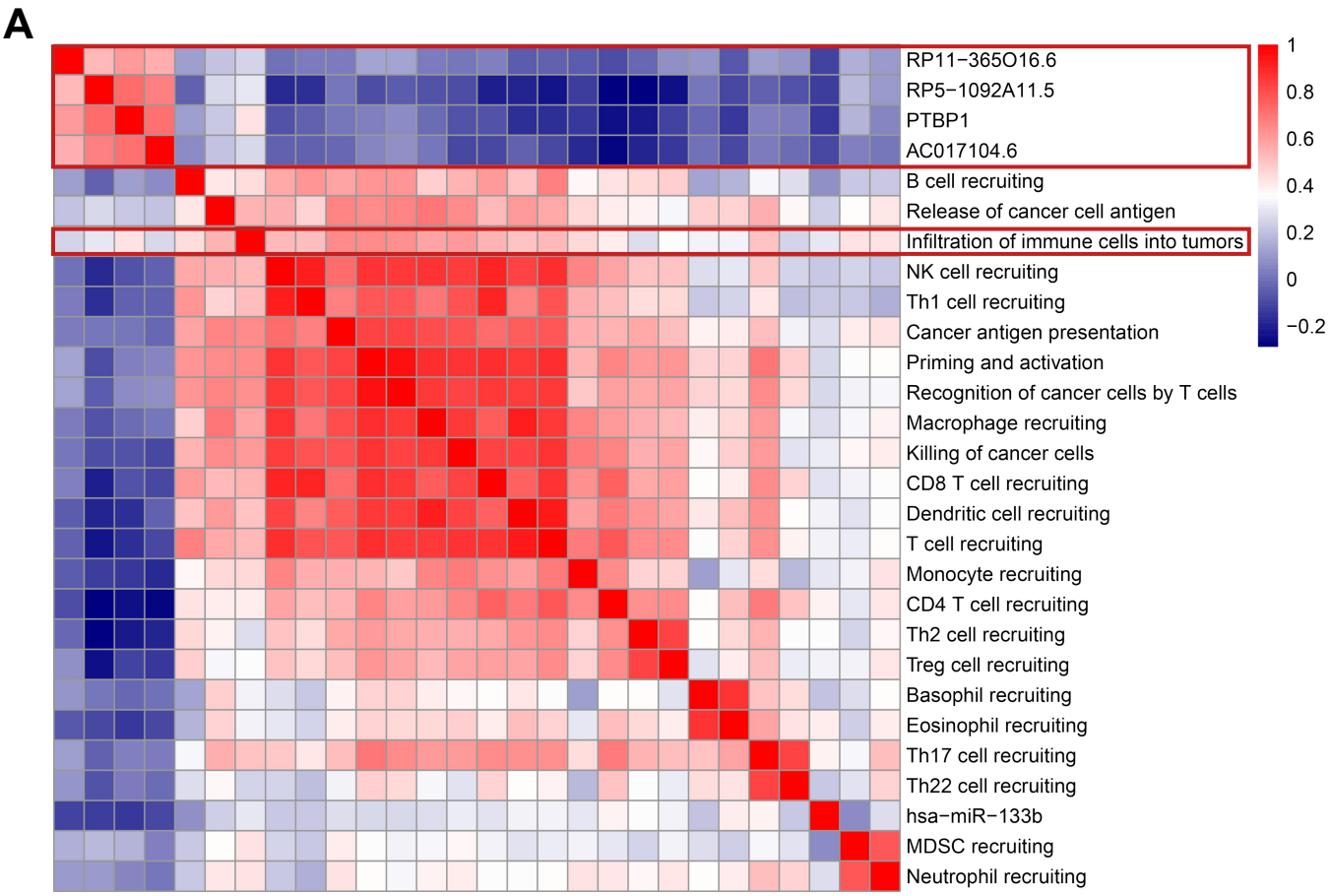

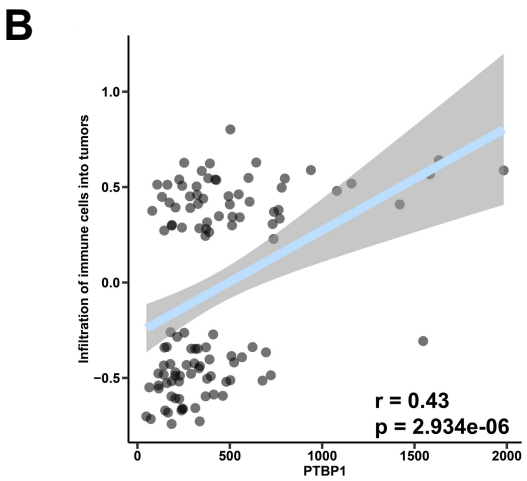

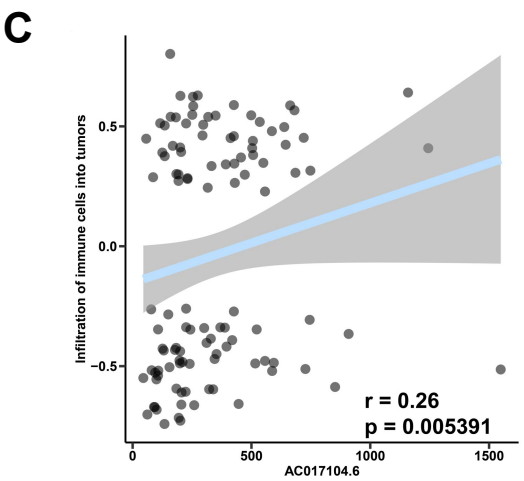

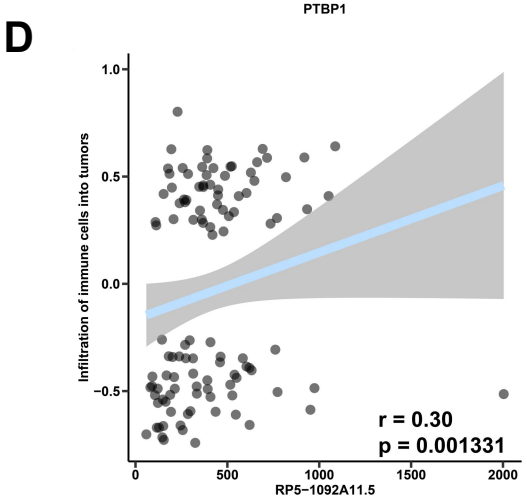

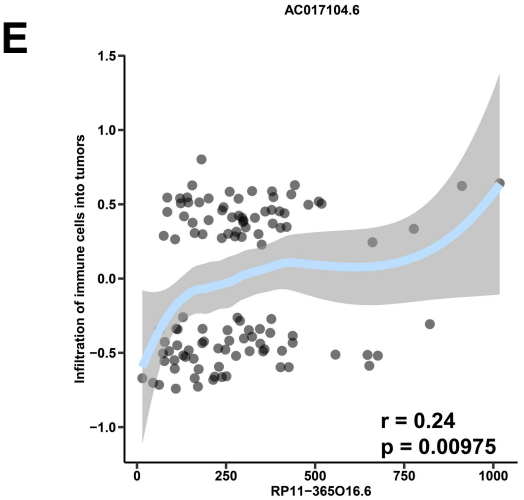

Supplementary Figure 11

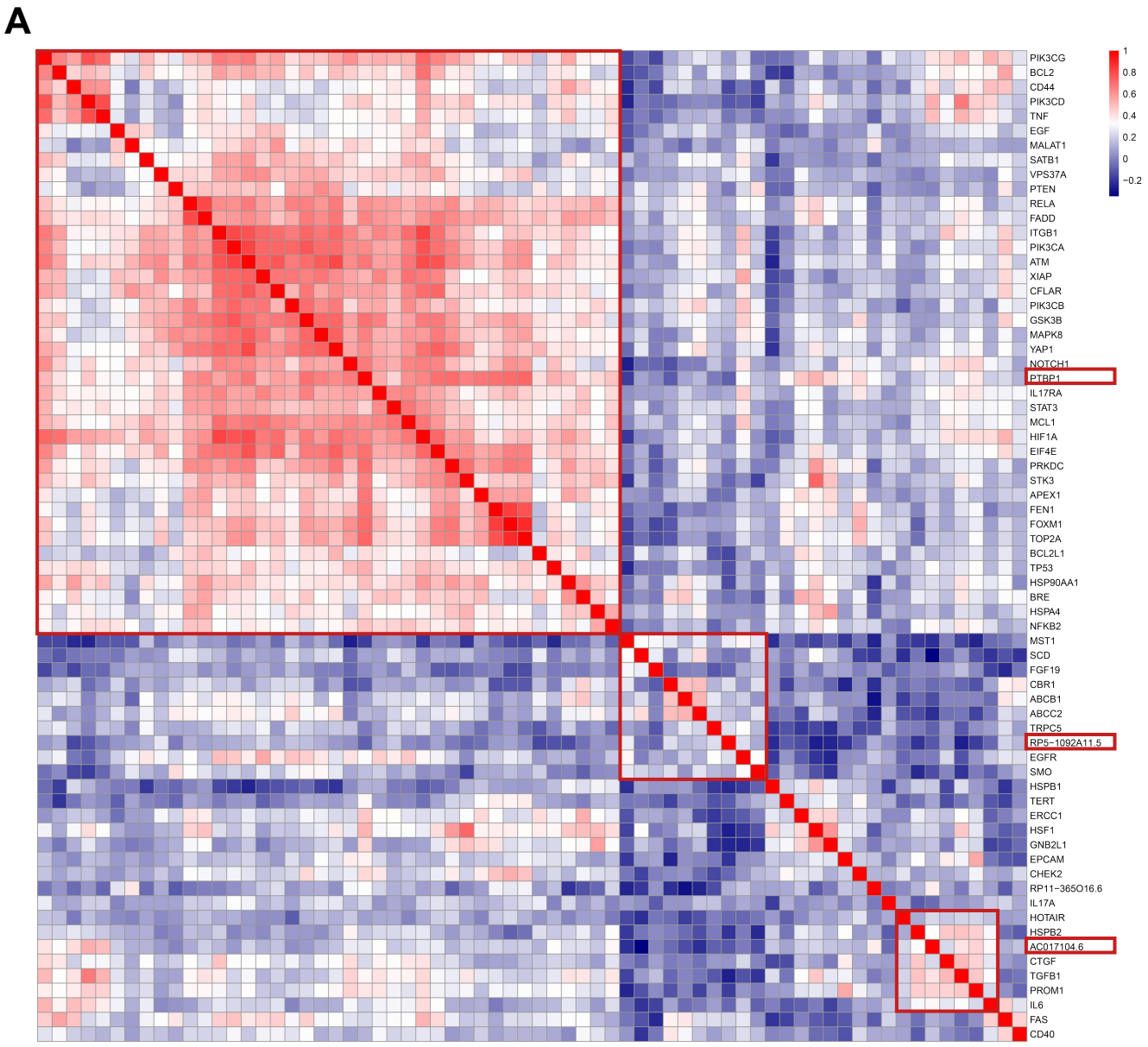

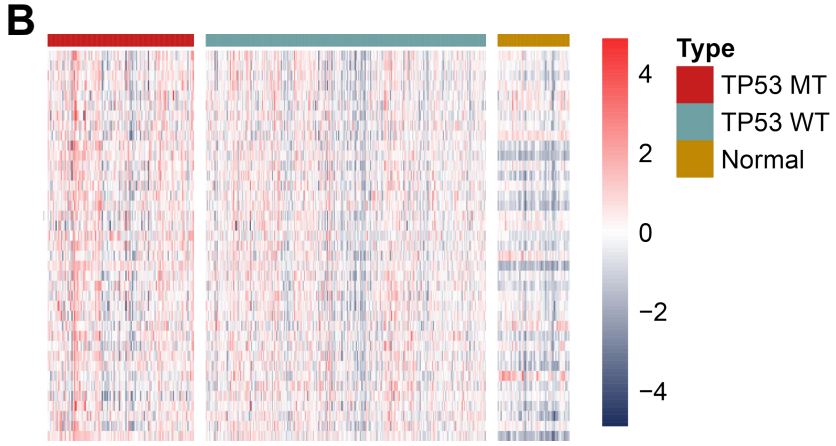

Supplementary Figure 12

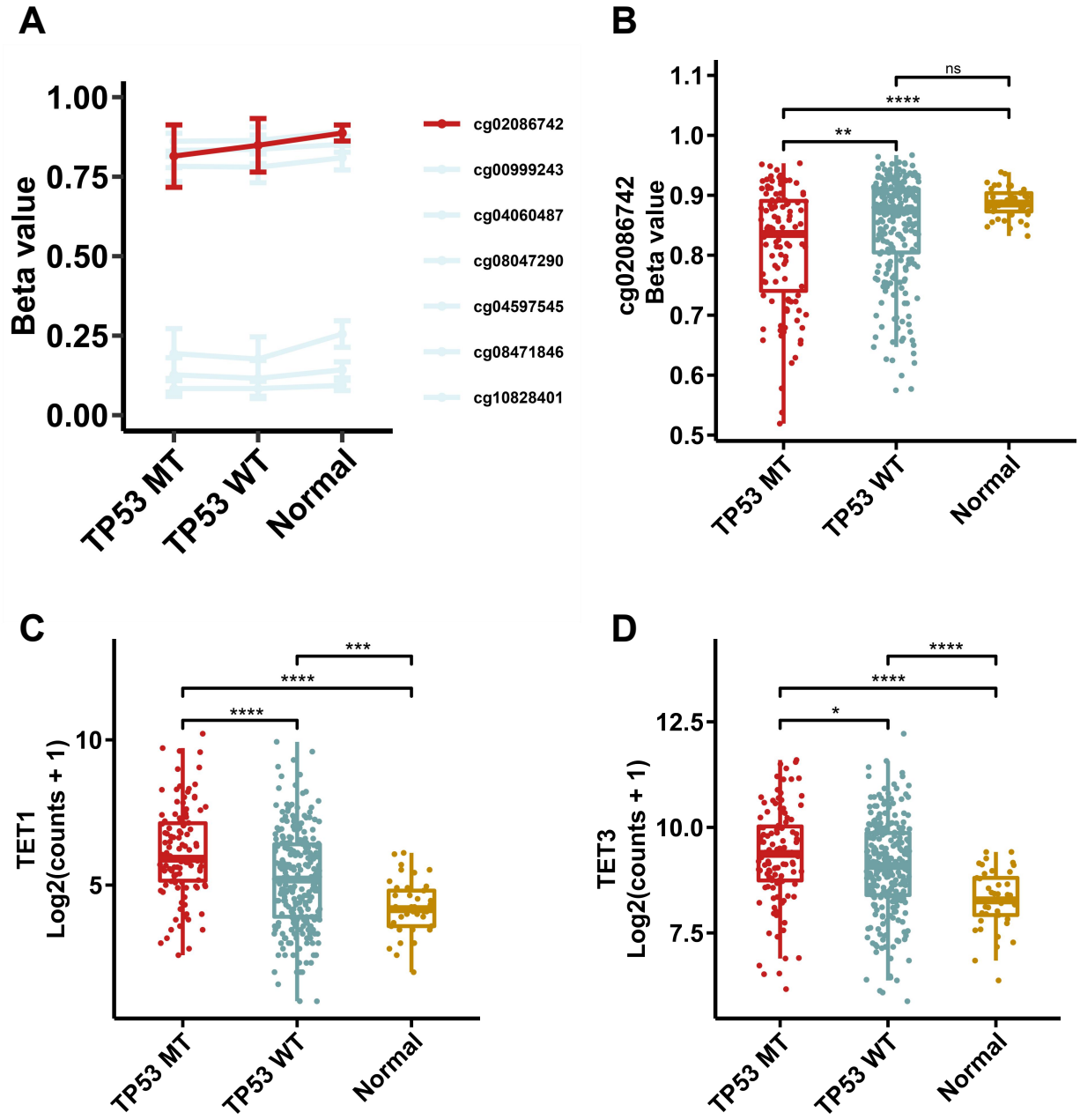

Supplementary Figure 13